Network Code Design for Orthogonal Two-hop Network with Broadcasting Relay: A Joint Source-Channel-Network Coding Approach

Roghayeh Joda and Farshad Lahouti

Wireless Multimedia Communications Laboratory

School of ECE, College of Engineering, University of Tehran

Email: [rjoda, lahouti]@ut.ac.ir, http://wmc.ut.ac.ir

Abstract

This paper addresses network code design for robust transmission of sources over an orthogonal two-hop wireless network with a broadcasting relay. The network consists of multiple sources and destinations in which each destination, benefiting the relay signal, intends to decode a subset of the sources. Two special instances of this network are orthogonal broadcast relay channel and the orthogonal multiple access relay channel. The focus is on complexity constrained scenarios, e.g., for wireless sensor networks, where channel coding is practically imperfect. Taking a source-channel and network coding approach, we design the network code (mapping) at the relay such that the average reconstruction distortion at the destinations is minimized. To this end, by decomposing the distortion into its components, an efficient design algorithm is proposed. The resulting network code is nonlinear and substantially outperforms the best performing linear network code. A motivating formulation of a family of structured nonlinear network codes is also presented. Numerical results and comparison with linear network coding at the relay and the corresponding distortion-power bound demonstrate the effectiveness of the proposed schemes and a promising research direction.

Index Terms

Network coding, relay network, wireless sensor network, minimum mean squared error estimation.

Preliminary reports on this research have appeared in IEEE Queen's Biennial Symposium on Communications, Kingston, ON, Canada, June 2008 and IEEE International Conference on Wireless Communications and Signal Processing, Nanjing, China, November 2009.

I. INTRODUCTION

A wireless sensor network consists of a large number of small, low cost and power constrained sensor nodes, which are spatially distributed and communicate through wireless channels. The nodes power limitation and the wireless propagation loss indicate that these nodes can communicate over short distances. Communications over longer ranges may be facilitated with multiple hops. In other words, the source signal is relayed by one or more nodes in the network and forwarded to the receiving nodes. We refer to a two-hop network with a single broadcasting relay as the TN-BR. In a TN-BR, utilizing the relay signal, each destination node intends to decode the signals transmitted by a certain subset of the sources. Two particular TN-BR scenarios are broadcast relay channel (BRC) (Fig. 1(a)) and multiple access relay channel (MARC) (Fig. 1(b)). In such networks, a dedicated relay assists reliable transmission by broadcasting an appropriate signal, based on a certain relaying scheme, to the destination(s) [1][2].

In this paper, we consider a special case of the TN-BR with N source nodes in which every source communicates with its intended destination(s) in a distinct orthogonal channel without interference. The relay is half duplex and listens to whatever the sources transmit; it then broadcasts to all the destinations in another orthogonal channel. We refer to such a network, with $N+1$ orthogonal channels, as orthogonal TN-BR (OTN-BR). In this orthogonal setting, a BRC may be viewed as one with several source-destination pairs with corresponding orthogonal channels and a dedicated broadcasting relay, referred to as the orthogonal multi-user channel with broadcasting relay (OMC-BR) [3]-[5]. This paper presents network code design at the relay for an OTN-BR with constrained resources and considers orthogonal MARC (OMARC) and OMC-BR as special cases.

Capacity achieving approaches in wireless channels with relay require substantial memory at the relay to accommodate inter-block encoding and large block sizes [6]-[8]. Though, in the context of complexity constrained wireless sensor networks simple channel codes and optimized memoryless mappings at the relay [9]-[12] are of practical interest. In [9] and [10], for a single source communicating a continuous signal to a single destination over a relay channel or through multi-hop relays, memoryless relay mappings maximizing the SNR at the destination are presented. In IEEE 802.15.4 [13], the widely popular standard for wireless sensor networks, in fact, no channel coding is considered. This implies that links are not practically error free and the

errors are to be tackled at higher layers of protocol stack. One option is to devise an automatic repeat request protocol at the link layer [14]. In this work, we take a joint source-channel-network coding approach to deal with the error at the presentation and network layers.

In a general network, network coding at the relay nodes may be considered for improved communications performance. In [15], it is shown that multicast capacity (maximum multicast rate) in an error free network can be achieved by network coding. In this setting, the intermediate nodes are allowed to decode and re-encode their incoming information. In [16], it is demonstrated that linear network coding with finite alphabet size can achieve the multicast capacity for communications over a network with error-free links. This corresponds to a separate design of network and channel coding, in the sense that perfect point to point channel codes render the links error-free from a network layer perspective. In [17], it is shown that source-network coding separation or channel-network coding separation is not optimal for non-multicast networks. In [18], it is shown that source and network coding separation is not optimal even for general multicast networks and that it is optimal only for networks with two sources and two receivers. Effective joint network-channel codes are presented for robust multicast over networks with noisy links in, e.g., [19]-[25].

In this paper, taking a joint source-channel-network coding approach for the OTN-BR, we present optimized network coding schemes at the relay for efficient reconstruction of the source signals at the destinations. In particular, we focus on resource constrained wireless networks, e.g., a wireless sensor network, where it is assumed that the mapping at the relay is memoryless and the channel coding is practically imperfect. First, a decoding scheme is presented for the minimum mean squared error (MMSE) reconstruction of signals transmitted from sources over the noisy channels of an OTN-BR at the destinations. As we shall demonstrate, in such a setting, the average reconstruction distortion at the OTN-BR destinations is decomposed into two parts referred to as the source distortion and the network distortion. The former is due to source coding and the latter primarily corresponds to the network, i.e., its channels, decoding and encoding (mapping) at the relay and decoding at the destinations. The network distortion is also influenced by the source coder output statistics. The objective is then to design a proper network code at the relay that minimizes the network distortion. This in turn lends itself to an efficient design scheme based on simulated annealing (SA), which results in a nonlinear network code at the relay. Taking insight of the resulting mappings, we next consider a motivating formulation of a

family of structured nonlinear network codes with substantially reduced design complexity. As a benchmark for comparisons, we also present performance cut-set bounds for OTN-BR.

Numerical results are provided demonstrating the superior performance of the proposed codes when compared to linear network coding. The outcomes are particularly inspiring as they demonstrate (i) the insufficiency of linear network coding in such wireless networks, (ii) a constructive approach to design nonlinear network codes and (iii) the effectiveness of the proposed joint source-channel-network coding schemes in complexity constrained wireless networks in comparison to the performance bounds.

The rest of this article is organized as follows. Following the preliminaries and the description of system model in Section II, Section III presents a MMSE decoder for OTN-BR. Next, in Section IV the distortion at the OTN-BR destinations is analyzed. In Section V, a method to design an optimized network code at the relay is presented and then a family of structured nonlinear network codes for the OTN-BR is suggested. Sections VI and VII present the separate source and channel-network coding bounds and the performance evaluations and comparisons, respectively. This article is concluded in Section VIII.

II. Preliminaries

A. Notation

The following notations are used in this paper. Capital letters, e.g., I, represent random variables and small letters, e.g., i, represent the realizations of random variables. We replace the probability $P(I = i)$ by $P(I)$ for simplicity. The vectors are shown bold faced, e.g., $\boldsymbol{I}$. The sets are identified by scripts, e.g., $\mathcal{A}$. For the set $\mathcal{A} \subset \mathcal{B}$, $\mathcal{A}^c$ denotes the complement of $\mathcal{A}$ in $\mathcal{B}$. We denote the sets of random variables $\{U_k : k \in \mathcal{A}\}$, $\{U_{m,k} : k \in \mathcal{A}\}$ and $\{U_{k,m} : k \in \mathcal{A}\}$ by $U_{\mathcal{A}}$, $U_{m,\mathcal{A}}$ and $U_{\mathcal{A},m}$, respectively.

B. OTN-BR

In an OTN-BR, there are N sources, M destinations and one relay. The sets $\mathcal{S} = \{1, ..., N\}$ and $\mathcal{D} = \{1, ..., M\}$, respectively indicate the set of sources and destinations. The transmitted signal of source $s \in \mathcal{S}$ is to be decoded at each of the nodes in $\mathcal{D}_s$. The subset of the sources that are to be decoded at the destination $d \in \mathcal{D}$ are denoted by $\mathcal{S}_d$.

In Section I, we presented OMARC and OMC-BR as particular instances of OTN-BR. In addition to these two networks, we also consider another instance of OTN-BR with two sources and three destinations, denoted by OTN-BR-(2,3) (Fig. 1(c)). While the developments in subsequent sections pertains to arbitrary OTN-BRs, we exemplify and assess the performance of the proposed code construction and decoding algorithms based on these three OTN-BR networks. In an OTN-BR-(2,3), the destination d, $d \in \{1, 2\}$ is to decode its corresponding source $s = d$, while the destination $d = 3$ is to decode the signals transmitted from both sources. Thus, in this network, $M = 3$, $N = 2$, $\mathcal{S}_{d=1} = \{1\}$, $\mathcal{S}_{d=2} = \{2\}$, $\mathcal{S}_{d=3} = \{1, 2\}$, $\mathcal{D}_{s=1} = \{1, 3\}$ and $\mathcal{D}_{s=2} = \{2, 3\}$. Furthermore, for an OMC-BR, $M = N$, $\mathcal{S}_d = \{d\} : d \in \mathcal{D}$ and $\mathcal{D}_s = \{s\} : s \in \mathcal{S}$, while for an OMARC, $M = 1$, $\mathcal{S}_{d=1} = \mathcal{S}$ and $\mathcal{D}_s = \{1\} : s \in \mathcal{S}$.

C. System Settings

At the source node s, $s \in \mathcal{S}$ the source signal X_s is scalar quantized with rate R_s, mapped to a codeword (index) and transmitted to the destination nodes $\mathcal{D}_s$. The number of quantization partitions (Voronoi regions) for source node s is equal to $L_s = 2^{R_s}$ and we refer to the partition I_s of this quantizer as V_{I_s}, where $I_s \in \mathcal{I}_s$, $\mathcal{I}_s = \{1, \ldots, L_s\}$. If the signal X_s belongs to V_{I_s}, the corresponding R_s bit index I_s is transmitted over a memoryless noisy channel orthogonal to those of other users. This is accomplished, e.g., based on a time multiplexing scheme [26] and BPSK modulation. In this case, when the source node s, $s \in \mathcal{S}$ transmits, the relay and destination nodes are in the receive mode; subsequently, the relay transmits and all the destination nodes are in the receive mode. Thus, the transmitted index I_s, $s \in \mathcal{S}$ is received over noisy channels at the relay and also at the corresponding destinations $\mathcal{D}_s$ as vectors $\boldsymbol{Y}_{r,s}$ and $\boldsymbol{Y}_{\mathcal{D}_s,s} = \{\boldsymbol{Y}_{d,s} : d \in \mathcal{D}_s\}$ each with R_s components, respectively.

As elaborated in Section I, focusing on a complexity constrained solution; we assume memoryless mappings at the relay. Therefore, the relay decodes the received vectors $\boldsymbol{Y}_{r,s}$, $s \in \mathcal{S}$ to the indexes $\hat{I}_s$, $s \in \mathcal{S}$ based on a maximum a posteriori (MAP) symbol decoding rule, i.e., $\hat{I}_s = \underset{I_s \in \mathcal{I}_s}{\operatorname{argmax}}\ P\left(I_s | \boldsymbol{Y}_{r,s}\right)$[1]. The relay then broadcasts the index $I_r = f(\hat{I}_{\mathcal{S}})$ with R_r bits to all destinations, where $I_r \in \mathcal{I}_r$, $\mathcal{I}_r = \{1, \ldots, L_r = 2^{R_r}\}$. Note that $f(\hat{I}_{\mathcal{S}})$ denotes an arbitrary (not necessarily linear) network coding function at the relay. The transmitted relay index I_r is

[1]Note that $|\mathcal{I}_s| = 2^{R_s}$ and the quantizer bit-rate R_s is limited, hence the decoding complexity is fairly small.

received at the destination node d, $d \in \mathcal{D}$ as $\boldsymbol{Y}_{d,r}$ with R_r components. Thus, the rate of the network code is defined as $R_{NC} \triangleq R_r / \sum_{s \in \mathcal{S}} R_s$.

Each of the communication channels is assumed memoryless, without intersymbol interference and described by the transition probabilities $P(\boldsymbol{Y}_{j,k}|I_k)$, where $(k, j) \in \mathcal{G}$ and

$$\mathcal{G} = \{(k, j) : k \in \mathcal{S}, j \in \mathcal{D}_k\} \cup \{(k, j) : k = r, j \in \mathcal{D}\} \cup \{(k, j) : k \in \mathcal{S}, j = r\}. \tag{1}$$

This may be motivated by the use of an interleaver or a scrambler at the physical layer. In this paper, we aim at designing the network code or mapping at the relay such that the average reconstruction distortion at the destinations is minimized.

D. Definitions

The developments in subsequent sections in general concern OTN-BR in arbitrary settings. However, the following particular scenarios are also considered in parts.

Definition 1: The "noiseless relay channels" corresponds to the scenario, where in an OTN-BR the channels from sources to the relay and also from the relay to the destinations are (almost) noiseless (high SNR). In this case, the source-destination channels can be noisy.

Definition 2: The "noiseless relay channels and very noisy source-destination channels" corresponds to the scenario, where in an OTN-BR the source-destination channels are very noisy and the channels from sources to the relay and also from the relay to the destinations are noiseless. When a channel is very noisy (low-end of SNR range), the output of the channel is (almost) independent of its input.

III. MMSE Decoding at OTN-BR Destinations

At each destination, the objective is to produce the minimum mean squared error estimation of the signals transmitted from its corresponding sources exploiting their dependencies with the signal received from the relay. According to the described system model, we take a joint source-channel-network coding approach that includes the effect of quantization as source coding. In line with the joint source-channel coding literature, the mean squared error (MSE) is a desired performance (distortion) criterion [27].

Proposition 1: In an OTN-BR destination node $d \in \mathcal{D}$, given $\boldsymbol{Y}_{d,\mathcal{S}_d}$ and $\boldsymbol{Y}_{d,r}$, respectively the received signals from sources $s \in \mathcal{S}_d$ and relay, the optimum MMSE reconstruction (estimation) of the transmitted source signal s is given by:

$$\begin{aligned}\hat{x}_{s,d} = g_s(\boldsymbol{Y}_{d,\mathcal{S}_d}, \boldsymbol{Y}_{d,r}) &= E\left[X_s|\boldsymbol{Y}_{d,\mathcal{S}_d}, \boldsymbol{Y}_{d,r}\right] \\ &= \frac{1}{K}\sum_{I_r}\sum_{I_{\mathcal{S}_d}} E\left[X_s|I_s\right] P(\boldsymbol{Y}_{d,\mathcal{S}_d}|I_{\mathcal{S}_d}) P(\boldsymbol{Y}_{d,r}|I_r) P(I_r|I_{\mathcal{S}_d}) P(I_{\mathcal{S}_d}),\end{aligned} \tag{2}$$

where

$$K = \sum_{I_r}\sum_{I_{\mathcal{S}_d}} P(\boldsymbol{Y}_{d,\mathcal{S}_d}|I_{\mathcal{S}_d}) P(\boldsymbol{Y}_{d,r}|I_r) P(I_r|I_{\mathcal{S}_d}) P(I_{\mathcal{S}_d}) \tag{3}$$

is a factor which normalizes the sum of probabilities to one.

Proof: In (2), $C_{I_s} \triangleq E[X_s|I_s]$, $s \in \mathcal{S}_d$, describes the codebook at the destination d corresponding to the source $s \in \mathcal{S}_d$. We have $P(\boldsymbol{Y}_{d,\mathcal{S}_d}|I_{\mathcal{S}_d}) = \prod_{s\in\mathcal{S}_d} P(\boldsymbol{Y}_{d,s}|I_s)$, and the terms $P(\boldsymbol{Y}_{d,s}|I_s)$, $s \in \mathcal{S}_d$ and $P(\boldsymbol{Y}_{d,r}|I_r)$ represent the channel transition probability for the channels from source s, and relay to destination d, respectively. The term $P(I_r|I_{\mathcal{S}_d})$ in (2) and (3) is given by

$$P(I_r|I_{\mathcal{S}_d}) = \sum_{\hat{I}_{\mathcal{S}}} P(I_r|\hat{I}_{\mathcal{S}}) P(\hat{I}_{\mathcal{S}_d}|I_{\mathcal{S}_d}) \prod_{j\in\mathcal{S}_d^c} P(\hat{I}_j), \tag{4}$$

in which $\hat{I}_{\mathcal{S}_d} = \{\hat{I}_s : s \in \mathcal{S}_d\}$ and $\hat{I}_s$ is the decoded index (symbol) at the relay corresponding to the index I_s emitted from the source s. The term $P(I_r|\hat{I}_{\mathcal{S}}) \in \{0,1\}$ corresponds to the mapping or the network code function $I_r = f(\hat{I}_{\mathcal{S}})$ at the relay. In (4), we have $P(\hat{I}_s) = \sum_{I_s} P(\hat{I}_s|I_s)P(I_s)$, where $P(\hat{I}_s|I_s)$, $s \in \mathcal{S}$ indicates the transition probability of the equivalent discrete source-relay channel. The proof is completed in Appendix A. ■

The value of C_{I_s} and $P(I_s)$, $s \in \mathcal{S}$ are acquired from the source coder and stored at every destination d, $d \in \mathcal{D}_s$. As the quantizers bit-rates are relatively small, this incurs a limited complexity. Given that the channel transition probabilities $P(\boldsymbol{Y}_{d,\mathcal{S}_d}|I_{\mathcal{S}_d})$ and $P(\boldsymbol{Y}_{d,r}|I_r)$, and the network code $f(\hat{I}_{\mathcal{S}})$ are available at the destination d, the RHS of (2) can be effectively computed.

The following two corollaries present Proposition 1 for OTN-BR in scenarios described by Definitions 1 and 2. These may be utilized to invoke simplified network code design procedures, as elaborated in Sections V and VII.

Corollary 1: In an OTN-BR with "noiseless relay channels", given $\boldsymbol{Y}_{d,\mathcal{S}_d}$ and I_r at the destination $d \in \mathcal{D}$, the MMSE estimation of the transmitted signal from the source $s \in \mathcal{S}_d$ is given by

$$\hat{x}_{s,d} = g_s^1(\boldsymbol{Y}_{d,\mathcal{S}_d}, I_r) \triangleq E\left[X_s|\boldsymbol{Y}_{d,\mathcal{S}_d}, I_r\right] = \frac{1}{K}\sum_{I_{\mathcal{S}}, f(I_{\mathcal{S}})=I_r} E\left[X_s|I_s\right] P(\boldsymbol{Y}_{d,\mathcal{S}_d}|I_{\mathcal{S}_d}) P(I_{\mathcal{S}}), \tag{5}$$

in which, K is a factor which normalizes the sum of probabilities to one.

Corollary 2: In an OTN-BR with "noiseless relay channels and very noisy source-destination channels", given I_r at the destination $d \in \mathcal{D}$, the MMSE estimation of the transmitted source signal $s \in \mathcal{S}_d$ is given by

$$\hat{x}_{s,d} = \hat{x}_s = g_s^2(I_r) \triangleq E\left[X_s | I_r\right] = \frac{1}{K} \sum_{I_{\mathcal{S}}, f(I_{\mathcal{S}})=I_r} E\left[X_s | I_s\right] P(I_{\mathcal{S}}), \tag{6}$$

in which, K is a factor which normalizes the sum of probabilities to one.
Using Proposition 1, obtaining the results in Corollaries 1 and 2 is straightforward.

IV. Distortion at Destinations

In this section, we investigate the average reconstruction distortion at the destinations in an OTN-BR. Specifically, we focus on how the distortion may be decomposed into its components to facilitate network code design at the relay. The average reconstruction distortion (MSE) at the destinations can be expressed as follows

$$\begin{aligned} D &= \frac{1}{\sum_{d=1}^{M} |\mathcal{S}_d|} \sum_{d=1}^{M} \sum_{s \in \mathcal{S}_d} E\left[X_s - \hat{X}_{s,d}\right]^2 \\ &= \frac{1}{\sum_{d=1}^{M} |\mathcal{S}_d|} \sum_{d=1}^{M} \sum_{s \in \mathcal{S}_d} \sum_{I_r} \sum_{I_{\mathcal{S}_d}} \int_{V_{I_{\mathcal{S}_d}}} \int_{\boldsymbol{Y}_{d,\mathcal{S}_d}} \int_{\boldsymbol{Y}_{d,r}} \left|X_s - g_s\left(\boldsymbol{Y}_{d,\mathcal{S}_d}, \boldsymbol{Y}_{d,r}\right)\right|^2 \\ &\times P\left(I_r | I_{\mathcal{S}_d}\right) P\left(\boldsymbol{Y}_{d,\mathcal{S}_d} | I_{\mathcal{S}_d}\right) P\left(\boldsymbol{Y}_{d,r} | I_r\right) P\left(X_{\mathcal{S}_d}\right) \mathrm{d}\boldsymbol{Y}_{d,\mathcal{S}_d} \mathrm{d}\boldsymbol{Y}_{d,r} \mathrm{d}X_{\mathcal{S}_d}, \end{aligned} \tag{7}$$

in which $\hat{X}_{s,d} = g_s\left(\boldsymbol{Y}_{d,\mathcal{S}_d}, \boldsymbol{Y}_{d,r}\right)$, $s \in \mathcal{S}$ is given in Proposition 1, $|\mathcal{S}_d|$ is the number of elements in $\mathcal{S}_d$, $V_{I_{\mathcal{S}_d}} = \{V_{I_k} : k \in \mathcal{S}_d\}$ denotes (Voronoi regions) quantization partitions I_k of sources $k \in \mathcal{S}_d$ and $P\left(I_r | I_{\mathcal{S}_d}\right)$ given in (4) represents the effect of source-relay channels, and decoding and network coding at the relay.

Proposition 2: The average distortion at the OTN-BR is equal to the sum of two terms as follows $D = D_{sources} + D_{network}$ in which

$$D_{sources} = \frac{1}{\sum_{d=1}^{M} |\mathcal{S}_d|} \sum_{d=1}^{M} \sum_{s \in \mathcal{S}_d} \sum_{I_s} \int_{V_{I_s}} \left|X_s - C_{I_s}\right|^2 P\left(X_s\right) \mathrm{d}X_s \tag{8}$$

and

$$D_{network} = \frac{1}{\sum\limits_{d=1}^{M} |\mathcal{S}_d|} \sum_{d=1}^{M} \sum_{s\in\mathcal{S}_d} \sum_{I_r} \sum_{I_{\mathcal{S}_d}} P\left(I_{\mathcal{S}_d}\right) \int\limits_{\boldsymbol{Y}_{d,\mathcal{S}_d}} \int\limits_{\boldsymbol{Y}_{d,r}} \left|C_{I_s} - g_s\left(\boldsymbol{Y}_{d,\mathcal{S}_d}, \boldsymbol{Y}_{d,r}\right)\right|^2 \times P\left(I_r|I_{\mathcal{S}_d}\right) P\left(\boldsymbol{Y}_{d,\mathcal{S}_d}|I_{\mathcal{S}_d}\right) P\left(\boldsymbol{Y}_{d,r}|I_r\right) \mathrm{d}\boldsymbol{Y}_{d,\mathcal{S}_d} \mathrm{d}\boldsymbol{Y}_{d,r}, \tag{9}$$

where $g_s\left(\boldsymbol{Y}_{d,\mathcal{S}_d}, \boldsymbol{Y}_{d,r}\right)$ and $P(I_r|I_{\mathcal{S}_d})$ are given in Proposition 1 and (4), respectively.

Proof: Replacing $|X_s - g_s\left(\boldsymbol{Y}_{d,\mathcal{S}_d}, \boldsymbol{Y}_{d,r}\right)|$ by $|X_s - C_{I_s} + C_{I_s} - g_s\left(\boldsymbol{Y}_{d,\mathcal{S}_d}, \boldsymbol{Y}_{d,r}\right)|$ in (7), we can write D as the sum of three terms, i.e., $D = D_{sources} + D_0 + D_{network}$, in which

$$D_{sources} = \frac{1}{\sum\limits_{d=1}^{M} |\mathcal{S}_d|} \sum_{d=1}^{M} \sum_{s\in\mathcal{S}_d} \sum_{I_r} \sum_{I_{\mathcal{S}_d}} \int\limits_{V_{I_{\mathcal{S}_d}}} \int\limits_{\boldsymbol{Y}_{d,\mathcal{S}_d}} \int\limits_{\boldsymbol{Y}_{d,r}} \left|X_s - C_{I_s}\right|^2 P\left(I_r|I_{\mathcal{S}_d}\right) \times P\left(\boldsymbol{Y}_{d,\mathcal{S}_d}|I_{\mathcal{S}_d}\right) P\left(\boldsymbol{Y}_{d,r}|I_r\right) P\left(X_{\mathcal{S}_d}\right) \mathrm{d}\boldsymbol{Y}_{d,\mathcal{S}_d} \mathrm{d}\boldsymbol{Y}_{d,r} \mathrm{d}X_{\mathcal{S}_d}, \tag{10}$$

$$D_0 = \frac{1}{\sum\limits_{d=1}^{M} |\mathcal{S}_d|} \sum_{d=1}^{M} \sum_{s\in\mathcal{S}_d} \sum_{I_r} \sum_{I_{\mathcal{S}_d}} \int\limits_{V_{I_{\mathcal{S}_d}}} \int\limits_{\boldsymbol{Y}_{d,\mathcal{S}_d}} \int\limits_{\boldsymbol{Y}_{d,r}} 2(X_s - C_{I_s}) \left(C_{I_s} - g_s\left(\boldsymbol{Y}_{d,\mathcal{S}_d}, \boldsymbol{Y}_{d,r}\right)\right) \times P\left(I_r|I_{\mathcal{S}_d}\right) P\left(\boldsymbol{Y}_{d,\mathcal{S}_d}|I_{\mathcal{S}_d}\right) P\left(\boldsymbol{Y}_{d,r}|I_r\right) P\left(X_{\mathcal{S}_d}\right) \mathrm{d}\boldsymbol{Y}_{d,\mathcal{S}_d} \mathrm{d}\boldsymbol{Y}_{d,r} \mathrm{d}X_{\mathcal{S}_d} \tag{11}$$

and

$$D_{network} = \frac{1}{\sum\limits_{d=1}^{M} |\mathcal{S}_d|} \sum_{d=1}^{M} \sum_{s\in\mathcal{S}_d} \sum_{I_r} \sum_{I_{\mathcal{S}_d}} \int\limits_{V_{I_{\mathcal{S}_d}}} \int\limits_{\boldsymbol{Y}_{d,\mathcal{S}_d}} \int\limits_{\boldsymbol{Y}_{d,r}} \left|C_{I_s} - g_s\left(\boldsymbol{Y}_{d,\mathcal{S}_d}, \boldsymbol{Y}_{d,r}\right)\right|^2 \times P\left(I_r|I_{\mathcal{S}_d}\right) P\left(\boldsymbol{Y}_{d,\mathcal{S}_d}|I_{\mathcal{S}_d}\right) P\left(\boldsymbol{Y}_{d,r}|I_r\right) P\left(X_{\mathcal{S}_d}\right) \mathrm{d}\boldsymbol{Y}_{d,\mathcal{S}_d} \mathrm{d}\boldsymbol{Y}_{d,r} \mathrm{d}X_{\mathcal{S}_d}. \tag{12}$$

Noting that the sources are independent and $\sum\limits_{I_s} \int\limits_{V_{I_s}} P(X_s)\mathrm{d}X_s = 1$, $D_{sources}$ in (10) is simplified to (8). Considering $\int\limits_{V_{I_s}} (X_s - C_{I_s}) P(X_s)\mathrm{d}X_s = 0$, it is straightforward to see that $D_0 = 0$. Finally, noting that $\int\limits_{V_{I_{\mathcal{S}_d}}} P(X_{\mathcal{S}_d})\mathrm{d}X_{\mathcal{S}_d} = P(I_{\mathcal{S}_d})$, we obtain $D_{network}$ as in (9). ■

As expected, the term $D_{sources}$ only depends on the distortion due to source coding (quantization) and is independent of the network code at the relay or of the channel. On the other hand, only the term $D_{network}$ depends on the channels and the network code at the relay. Hence, we design the network code such that $D_{network}$ is minimized. As evident, $D_{network}$ also depends on source coder output statistics and MMSE decoding of the source signals at destinations. Therefore, the design takes a joint source-channel-network coding approach.

The following two corollaries present Proposition 2 for OTN-BR in scenarios described by Definitions 1 and 2. These may be utilized to invoke simplified network code design procedures, as elaborated in Sections V and VII.

Corollary 3: In an OTN-BR with "noiseless relay channels", $D_{network}$ is given by:

$$D_{network} = \frac{1}{\sum\limits_{d=1}^{M} |\mathcal{S}_d|} \sum_{d=1}^{M} \sum_{s \in \mathcal{S}_d} \sum_{I_{\mathcal{S}}} P\left(I_{\mathcal{S}}\right) \int\limits_{\boldsymbol{Y}_{d,\mathcal{S}_d}} \left| C_{I_s} - g_s^1\left(\boldsymbol{Y}_{d,\mathcal{S}_d}, I_r = f(I_{\mathcal{S}})\right)\right|^2 P\left(\boldsymbol{Y}_{d,\mathcal{S}_d} | I_{\mathcal{S}_d}\right) \mathrm{d}\boldsymbol{Y}_{d,\mathcal{S}_d}, \tag{13}$$

where $g_s^1(\boldsymbol{Y}_{d,\mathcal{S}_d}, I_r)$, $s \in \mathcal{S}$ is given in Corollary 1.

Corollary 4: In an OTN-BR with "noiseless relay channels and very noisy source-destination channels", $D_{network}$ is given by:

$$D_{network} = \frac{1}{\sum\limits_{d=1}^{M} |\mathcal{S}_d|} \sum_{d=1}^{M} \sum_{s \in \mathcal{S}_d} \sum_{I_{\mathcal{S}}} P\left(I_{\mathcal{S}}\right) \left| C_{I_s} - g_s^2\left(I_r = f(I_{\mathcal{S}})\right)\right|^2, \tag{14}$$

where $g_s^2(I_r)$, $s \in \mathcal{S}$ is given in Corollary 2.

V. Code Design at the Relay: Implementation and Complexity Considerations

As described in Section II-C, the relay MAP decodes the received signals $\boldsymbol{Y}_{r,s}$, $s \in \mathcal{S}$ to the indexes $\hat{I}_{\mathcal{S}} = \{\hat{I}_s : s \in \mathcal{S}\}$ and then broadcasts the network coded index $I_r = f(\hat{I}_{\mathcal{S}})$ to the destinations. At the relay, the network code $f(\hat{I}_{\mathcal{S}})$ is designed such that the average reconstructed signal distortion at the destinations is minimized. Since only $D_{network}$ depends on the network code at the relay, the goal is to minimize $D_{network}$ as defined in (9), (13) or (14). To this end, an exhaustive search to identify the optimal code at the relay requires $2^{R_1} \times \ldots \times 2^{R_N} \times 2^{R_r}$ tests of all combinations. Thus in the following, targeting an efficient solution, we first devise an approach based on simulated annealing and then inspired by the results attempt to formulate a structured network code.

A. Network Code Design at the Relay: An Approach based on Simulated Annealing

Simulated annealing is an iterative algorithm that belongs to the class of randomized algorithms for solving combinatorial optimization problems. Given the current state (here network code), the next candidate state in SA is created with certain level of randomness, based on a so-called perturbation scheme. To avoid sticking in local minima, a candidate state with higher cost may also be probabilistically selected as the new state [28]. The SA converges in probability to a global minimum if a proper perturbation scheme and a suitably slow cooling schedule are used

[28]. The two govern the possible improvements to the code in each iteration and the number of iterations, respectively. In particular, if the initial temperature T_0 is sufficiently large, a cooling schedule described by $T_k = c/\log(k+1)$, guarantees such a convergence [28], where c is a positive constant and T_k is the temperature after k temperature drops. The SA is previously used for index assignment in robust source coding [28] and also for designing source and channel codes in [29]. An alternative binary switching scheme is used in [30] for source-optimized channel coding in point-to-point digital transmission.

We consider a $2^{R_1} \times \ldots \times 2^{R_N}$ lookup-table (codebook) at the relay in which each element indicates the mapping of codewords (indexes) $\left(\hat{I}_1, \hat{I}_2, \ldots, \hat{I}_N\right)$ received from the sources to an index at the output of the relay. The proposed SA-based algorithm to design this code at the relay is described below.

1) Set an initial appropriate high temperature $T = T_0$.
2) If this is the first iteration, initialize the lookup-table randomly. Otherwise, generate a test code by perturbing the current one. Perturbation is accomplished by changing the value of a certain table element to that of one random element among its adjacent neighbors. The element for perturbation is chosen in order, e.g., row-wise, in subsequent iterations.
3) Calculate $D_{network}$ using Proposition 2 (resp. Corollary 3 or 4). Compute the change in $D_{network}$ in comparison to that in previous iteration ($\triangle D$).
4) If $\triangle D < 0$, then the perturbed code is adopted. Otherwise, it is only chosen with probability $\exp(\frac{-\triangle D}{T})$.
5) Iterate by going to step 2, until the code is updated for a sufficient number of times or a maximum number of iterations is reached.
6) Lower the temperature. If the temperature is below a specified value or the relative change in $D_{network}$ is insignificant, stop; otherwise go to step 2. The cooling schedule adopted here is $T_k = \alpha T_{k-1}$, $0 < \alpha < 1$, as in [28][29], which allows for a faster design process.

When the algorithm terminates, the code design process is completed and the resulting code may be used for operations. Thus, the main complexity remains at the design procedure for the network code at the relay.

Remark 1: To design nonlinear network codes as described, particular assumptions on channel conditions may be made to simplify the design procedure. This is incorporated in step 3 of the algorithm, where Corollary 3 or 4 may be utilized instead of Proposition 2. This provides

performance versus design complexity trade-offs, as assessed in various channel conditions in Section VII.

Remark 2: Although, the proposed network code design algorithm is devised for a general OTN-BR, where soft outputs may also be available at the destinations, to speed up the design procedure, one could consider equivalent hard-decided received signals. Naturally, in this case the integrals in (9), (13) or (14) are replaced with summations.

Example 1: As an example of the network code design, we here consider an OTN-BR with two sources, when the source signals are Gaussian and $R_1 = R_2 = R$. For $R_r = R = 3$, the network code is an 8×8 lookup-table, where one of 8 codewords (indexed 0 to 7) is assigned to each of its elements. One such code obtained via the proposed SA-based scheme is presented in Fig. 2(a). This code is clearly nonlinear as for example, for $[I_1, I_2] = [1, 1]$ and $[\acute{I}_1, \acute{I}_2] = [2, 4]$, $f(I_1, I_2) = 6$ and $f(\acute{I}_1, \acute{I}_2) = 0$, while $f(I_1 \oplus \acute{I}_1, I_2 \oplus \acute{I}_2) = 0$. Of course, the network code f is linear if and only if $\forall I_j, \acute{I}_j \in \mathcal{I}_j$, $0 \leq j \leq N-1$, $f(I_1, \ldots, I_N) \oplus f(\acute{I}_1, \ldots, \acute{I}_N) = f(I_1 \oplus \acute{I}_1, \ldots, I_N \oplus \acute{I}_N)$, in which $\oplus$ denotes summation in $GF(2^{R_r})$.

B. Structured Network Code

As stated, our experiments demonstrate that the network codes obtained for the relay based on the proposed approach in Section V-A are nonlinear. Motivated by these results, here we attempt to formulate a structured nonlinear network code. This provides a closed form expression of the network code at relay, and as we shall demonstrate substantially reduces the design complexity. It is noteworthy that there is only very limited reports in the literature on the theory of nonlinear (channel) codes, e.g., [31].

Consider the proposed network code in Fig. 2(a) designed for an OTN-BR with two sources and $R_r = R = 3$, $R_{NC} = \frac{1}{2}$. As evident, there are regions or clusters with the same codeword which partition the codebook. Our research indicate that the performance of the code is primarily affected by the partitioning and not by the exact codeword (index) assigned to each partition. Based on these observations, in Fig. 2(b) for the two source OTN-BR, a structured network code is proposed based on a partitioning of the network codebook (lookup-table at the relay). As a possible extension to the case of OTN-BR with N sources with the same network coding rate, we consider the setting where the mapping of the first dimension and any other dimension follows the same partitioning as that in Fig. 2(b). The resulting family of structured network

codes $f(\hat{I}_1,\dots,\hat{I}_N)$ may be formulated as follows.

$$f\left(\hat{I}_1,\dots,\hat{I}_s,\dots,\hat{I}_N\right)=\begin{cases} a_{k_2,\dots,k_N} & 0\le \hat{I}_1<2\ ,\ k_{s\neq 1}=\hat{I}_s\circ 2^{R_s-1}: k_{s\neq 1}\in\{0,1\} \\ b_{k_1,k_2,\dots,k_N} & 2\le \hat{I}_1<2^{R_1}-2,\ k_1=\left\lfloor\frac{\hat{I}_1-2}{4}\right\rfloor,\ k_{s\neq 1}=\left\lfloor\frac{\hat{I}_s}{2^{R_s-2}}\right\rfloor: \\ & \quad k_1\in\{0,\dots,2^{R_1-2}-1\}\ ,\ k_{s\neq 1}\in\{0,\dots,3\}, \\ e_{k_2,\dots,k_N} & 2^{R_1}-2\le \hat{I}_1<2^{R_1},\ k_{s\neq 1}=\hat{I}_s\circ 2^{R_s-1}: k_{s\neq 1}\in\{0,1\} \end{cases} \tag{15}$$

where, the operation $\circ$ is defined as $\hat{I}_s\circ 2^{R_s-1}=\begin{cases}0 & \text{if}\quad 0\le\hat{I}_s<2^{R_s-1}\\ 1 & \text{otherwise.}\end{cases}$. In (15), $a_{k_2,\dots,k_N}$, $b_{k_1,k_2,\dots,k_N}$, $e_{k_2,\dots,k_N}\in\mathcal{I}_r$ are 2^{R_r} distinct indices. As the partitioning is now fixed according to (15), the design is now simplified to assigning the values of these indices, which may be handled by a SA-based algorithm with substantially smaller complexity. Our experiments (reported in part in Section VII) reveal the efficiency of the proposed code structure and only a small performance gap with the (unstructured) code produced by the presented algorithm in Section V-A. Noting the definition of network coding rate R_{NC} and utilizing (15) for $R_s=R\ \forall s\in\mathcal{S}$, we have $R_{NC}=\left\lceil\log_2\left(4\times 2^{N-2}+\left(2^R-4\right)\times 4^{N-2}\right)\right\rceil/NR$, which as desired is nearly $\frac{1}{2}$ for $R\in\{2,3,4\}$ and $N<5$.

VI. Separate Source Channel-Network Coding Bound

In this section, we present performance bounds by combining the rate-distortion function due to source coding with the capacity upper-bound, due to the cut-set bound for wireless networks under consideration. The latter corresponds to joint channel-network coding. Therefore, we refer to the bounds thus derived as the separate source and channel-network coding bound, which is naturally obtained assuming large block lengths.

In the following, we first present a cut-set upper bound on the achievable rates $R_{c,s}$ (bits per channel use - due to joint channel-network coding) in a Gaussian OTN-BR for communications between the source node s and the corresponding destination nodes, $\mathcal{D}_s$. In a Gaussian OTN-BR, each link is modeled as an independent additive white Gaussian noise channel, where the noise is zero mean with variance $\sigma^2_{n,m},\forall(n,m)\in\mathcal{G}$ (refer to (1) for the definition of $\mathcal{G}$). Considering orthogonality of channels based on time multiplexing, the sources and the relay each transmit in a fraction of time T, i.e., $\lambda_1 T,\dots,\lambda_N T$ and $\left(1-\sum_{s\in\mathcal{S}}\lambda_s\right)T$, respectively. Suppose that the

sources and the relay are subject to the average power constraints $P_1, \ldots, P_N$ and P_r. Thus, these nodes can transmit respectively with the average powers $\acute{P_1} = P_1/\lambda_1, \ldots, \acute{P_N} = P_N/\lambda_N$ and $\acute{P_r} = P_r/\big(1 - \sum_{s\in\mathcal{S}} \lambda_s\big)$ during their corresponding transmission periods.

Proposition 3: For a Gaussian OTN-BR with N source and M destination nodes, the cut-set upper bound for the rates $(R_{c,1}, \ldots, R_{c,s}, \ldots, R_{c,N})$ is given by

$$\sum_{\substack{s\in\mathcal{F}:\\ \mathcal{F}\subset\mathcal{S}}} R_{c,s} \le \max_{\substack{0\le\lambda_{\acute{s}}\le 1\\ \acute{s}\in\mathcal{S}}} \min\Bigg\{\sum_{\acute{s}\in\mathcal{F}} \lambda_{\acute{s}}\frac{1}{2}\log_2\Bigg(1+\sum_{d\in\{\mathcal{D}_{\acute{s}}\}}\frac{\acute{P}_{\acute{s}}}{\sigma^2_{\acute{s},d}}+\frac{\acute{P}_{\acute{s}}}{\sigma^2_{\acute{s},r}}\Bigg), \sum_{\acute{s}\in\mathcal{F}} \lambda_{\acute{s}}\frac{1}{2}\log_2\Bigg(1+\sum_{d\in\{\mathcal{A}\cap\mathcal{D}_{\acute{s}}\}}\frac{\acute{P}_{\acute{s}}}{\sigma^2_{\acute{s},d}}\Bigg)$$
$$+\Bigg(1-\sum_{\acute{s}\in\mathcal{S}}\lambda_{\acute{s}}\Bigg)\frac{1}{2}\log_2\Bigg(1+\sum_{d\in\mathcal{A}}\frac{\acute{P}_r}{\sigma^2_{r,d}}\Bigg) : \forall\mathcal{A}\subset\mathcal{D}_{\mathcal{F}},\ \mathcal{S}_{\mathcal{A}}\cap\mathcal{F}=\mathcal{F}\Bigg\} \tag{16}$$

Proof: We consider $\mathcal{F}$ as a subset of sources, i.e., $\mathcal{F} \subset \mathcal{S}$. A set of destinations, whose every member intends to decode all the sources in $\mathcal{F}$ is denoted by $\mathcal{A}$, $\mathcal{A} \subset \mathcal{D}_{\mathcal{F}}$. The cut C_1, is considered as that crossing only the outgoing channels from $\mathcal{F}$. On the other hand, the cut crossing the incoming channels to $\mathcal{A}$ and also including only the outgoing channels from the relay and $\mathcal{F}$ is denoted by C_2. Using max-flow min-cut theorem for the OTN-BR, we see that the maximum transmission sum-rate by the sources in $\mathcal{F}$ is equal to the minimum of information flow across the cut C_1 or the cuts C_2 corresponding to all possible subsets $\mathcal{A}$. As evident in RHS of (16), the first term corresponds to the cut C_1 and the next term is related to the cuts C_2. The complete proof of Propositions 3 is provided in Appendix B. ■

For a Gaussian source with variance σ_s^2 and a source coding rate of R_s bits per source sample, the distortion-rate function $D(R_s)$ is equal to $\sigma_s^2 2^{-2R_s}$ [6]. Considering separate source and channel-network coding, we have

$$D(bR_{c,s}) = \sigma_s^2 2^{-2bR_{c,s}}, \tag{17}$$

where b denotes the number of channel uses per source sample. Thus, equation (17) in conjunction with Proposition 3, presents a distortion-power function that serves as a performance bound in the sequel.

We now consider Proposition 3 in a special case for a Gaussian OTN-BR-(2,3) in a symmetric network setting. A Gaussian OTN-BR is symmetric when $\sigma^2_{s,d} = \sigma^2_{sd}$, $\sigma^2_{s,r} = \sigma^2_{sr}$, $\sigma^2_{r,d} = \sigma^2_{rd}$ and $P_s = P,\ s \in \mathcal{S},\ d \in \mathcal{D}$. We thus have $R_{c,s} = R_c\ \forall s \in \mathcal{S}$.

Corollary 5: For a symmetric Gaussian OTN-BR-(2,3), the cut-set upper bound on the rates $R_{c,s} = R_c,\ s \in \mathcal{S}$ is given by

$$R_c \leq \max_{0 \leq \lambda \leq \frac{1}{2}} \min \left\{ \lambda \frac{1}{2} \log_2 \left(1 + \frac{2P}{\lambda \sigma_{sd}^2} + \frac{P}{\lambda \sigma_{sr}^2} \right), \right.$$
$$\left. \lambda \frac{1}{2} \log_2 \left(1 + \frac{P}{\lambda \sigma_{sd}^2} \right) + (1-2\lambda) \frac{1}{4} \log_2 \left(1 + \frac{P_r}{(1-2\lambda)\sigma_{rd}^2} \right) \right\}. \tag{18}$$

Following the approach described above, we can use (17) and obtain a distortion-power function for a symmetric Gaussian OTN-BR(2,3). This provides a performance bound for comparisons in Section VII. The bounds for OMARC and OMC-BR can be obtained in a similar way.

VII. Performance Evaluation

Consider a symmetric Gaussian OTN-BR with N source nodes producing independent Gaussian distributed signals with zero mean and unit variance, that are to be transmitted to the corresponding destinations. Each of these continuous signals is quantized using a 2^R level Lloyd-Max quantizer. The resulting quantization index is represented by a binary codeword. Each binary codeword is BPSK modulated and transmitted through a Gaussian channel. The network code at the relay is described by a $2^R \times 2^R$ and $2^R \times 2^R \times 2^R$ lookup-table for $N = 2$ and $N = 3$, respectively. To obtain network codes of rate (approximately) $\frac{1}{2}$, the relay transmission rate is selected as $R_r = R$ for $N = 2$, and $R_r = 5$ bits for $N = 3,\ R = 3$.

At the relay, the received codewords from the sources are (symbol) MAP decoded and are combined using the proposed nonlinear network coding. Hence, we refer to them as decode and nonlinear network coding (DNNC) schemes and denote them by DNNC-Structured, DNNC-C3 and DNNC-C4 indicating, as described in Section V, the design based on the structured network code, or Corollaries 3 and 4, respectively. For comparison, we consider MAP decoding followed by classic linear network coding at the relay and refer to it as decode and linear network coding (DLNC). In this case, the binary codewords are represented and linearly combined in $GF(2^{R_r})$ with coefficients searched and selected to minimize the average distortion at the destinations. The code thus obtained is referred to as the best performing linear network code.

For the performance evaluations of symmetric OTN-BRs in the following, the signal to noise ratio of the channel from any source to any of its corresponding destination nodes is denoted by SNR_{sd}^{design} and SNR_{sd}, during the design and operations, respectively. In the same direction,

SNR_{rd} and SNR_{sr}, respectively demonstrate the SNRs of the relay-destination channels and the source-relay channels during the operations. The average reconstruction signal SNR (RSNR), i.e., $\frac{1}{N}\sum_{i=1}^{N}\frac{E\left[X_i^2\right]}{D}$, where D is obtained from (7), is used as the performance criterion.

A. Basic Comparisons

Figs. 3 and 4 respectively, present the performance of an OMC-BR and an OMARC, with two sources, $R = 3$, $R_{NC} = \frac{1}{2}$ and $SNR_{sd} = -3\text{dB}$. These figures and the results for the OTN-BR-(2,3) (not reported here) demonstrate that the proposed DNNC schemes substantially outperform the DLNC scheme. Specifically, a RSNR gain of about 4dB is achieved for all considered networks, when the source-relay and the relay-destination channels are of good quality.

The DNNC-C4 (with the code in Fig. 2(a)) is designed assuming very noisy source-destination channels and is simpler to design in comparison to DNNC-C3. Both DNNC-C3 and DNNC-C4, are designed assuming noiseless relay-destination channels. In such settings, however, as evident in Figs. 3 to 5, DNNC-C3 outperforms DNNC-C4.

Examining the performance of the proposed DNNC-C3 scheme designed for SNR_{sd}^{design} of -3dB and 1dB in Figs. 3 to 5 demonstrates that, as expected, when the operating channel conditions are closer to the design setting, a higher performance is obtained. It is interesting to note, however, that the sensitivity of the performance to a mismatch of design and operations channel SNRs is insignificant. Our experiments over severely asymmetric networks indicate that the proposed network code in DNNC-C3 is designed to further assist the communication of source(s) with lower source-destination channel SNR.

Also, comparing Figs. 4 and 5, it is evident that when the quality of the source-destination channels improves, as expected, the RSNR is enhanced and ultimately reaches that of a 3-bit Lloyd Max quantizer ($\sim 15\text{dB}$). For noisy source-destination channels, the RSNR does not reach this limit even if the source-relay and the relay-destination channels are noiseless. This is due to the fact that the network coding at the relay is not a one-to-one mapping, and as expected, the corresponding relay signal is only meant to assist the source-destination transmission. In the current example, the relay receives $R_1 = 3$ and $R_2 = 3$ bit codewords from sources 1 and 2, respectively, while produces only one $R_r = 3$ bit codeword.

In our studies, we have also examined another scheme (not reported here), which is referred to as estimate and forward nonlinear network coding (ENNC). In ENNC, the source signal

transmitted by each source is first estimated at the relay using an MMSE decoder. Subsequently, the estimated source signals at the relay are mapped to an output codeword using an optimized vector quantization scheme. According to our simulations, the ENNC provides only a limited gain over the DNNC at the cost of increased complexity.

B. Effects of Rates of Network Coding and Quantization

Fig. 6 presents the performance of OMC-BR network with $N = 3$, for different network coding schemes and rates. The operation source-destination channel SNRs are set to $SNR_{sd} = -3\text{dB}$. It is observed that, with $R = 3$, $R_r = 5$ and $R_{NC} = \frac{1}{2}$, the proposed DNNC schemes achieve a gain of about 4dB in the RSNR compared to DLNC. Therefore, noting Figs. 3, 4 and 6, it is evident that similar gains are achieved in the considered networks with $N = 2$ and $N = 3$ for a given source-destination channel SNR, and rates of network coding and quantization. Fig. 6 also depicts the performance of the DLNC and the proposed DNNC schemes for $R_r = R = 3$, $R_{NC} = \frac{1}{3}$. As expected, for a given quantization rate, the performance gain provided by the DNNC schemes is greater, when the network code rate R_{NC} is larger.

Figs. 7 and 8, respectively depict the resulting average distortion in an OMARC and an OTN-BR-(2,3) as a function of rate for $R \in \{2, 3, 4\}$. It is observed that the proposed DNNC scheme provides a larger performance gain with respect to DLNC, when the quantization rate is greater.

C. Performance of the Proposed Structured Nonlinear Network Code

The performance of the proposed structured nonlinear network code is depicted in Figs. 3 to 6. This code is presented in Fig. 2(b) for $N = 2$ and in (15) for arbitrary N. As evident, the structured network code performs closely similar to DNNC-C3 especially for high quality relay-destination channels. However, this performance is obtained with much smaller design complexity. Our experiments indicate that the nearly symmetric structure of the proposed structured network code leads to almost identical performance at different receivers over a symmetric network. For example, in a symmetric OMC-BR with $N = 3$, $SNR_{sd} = -3\text{dB}$ and $SNR_{rd} = 7\text{dB}$, the average RSNR at the destinations 1, 2 and 3 is 8.42dB, 8.74dB and 8.84dB, respectively.

Considering symmetric network settings and the definition of the average distortion in (7), each of the proposed DNNC schemes in the three OTN-BR instances of interest provides the

same performance for given SNR_{sd} and SNR_{rd}. This issue is evident in the simulation results depicted in Figs. 3-5, 7 and 8. However, DLNC provides a better performance in OMARC in comparison to other considered networks as it is seen in Figs. 7 and 8.

D. Distortion Power Trade-off

Fig. 9 demonstrates the trade-off of average distortion and power of the sources (SNR_{sd}) for an OTN-BR-(2,3). In this figure, the performance of the proposed DNNC with structured nonlinear network coding and DLNC are depicted together with the separate source and channel-network coding bound obtained from Corollary 5 for comparison. In Fig. 9, it is seen that the proposed DNNC with structured network code compared to DLNC reduces the gap to the bound by more than 50%. It is also evident in this figure that, (i) for high SNR_{sd} both DNNC and DLNC result in identical residual distortion equal to that of a 3-bit Lloyd-Max quantizer, that is due to source coding; and (ii) an improved SNR_{rd} enhances the performance gain provided by the proposed DNNC scheme. Our simulation results (not reported here) confirm similar observations for the OMARC and OMC-BR.

VIII. Conclusions

In this paper, network code design for the orthogonal two-hop network with broadcasting relay and constrained complexity was investigated. Taking a joint source-channel-network coding approach, the network code at the relay was designed to minimize the average distortion at the destinations. Decomposing the distortion into its components enabled the development of an effective network code design algorithm based on simulated annealing. The resulting network code is nonlinear and outperforms the best performing linear network codes. This indicates the insufficiency of linear network coding in complexity constrained wireless networks with a MMSE design criteria. The results also show that the sensitivity of the proposed nonlinear network code to a mismatch of design and operations channel SNRs is insignificant and the performance gain provided by the nonlinear code compared to the linear code is greater, when the network code rate is larger. In comparison to the separate source and channel-network coding bound, the proposed nonlinear network coding at the relay in contrast to the linear code reduces the gap to the bound by more than 50%. This fact indicates the effectiveness of the proposed decode and nonlinear network coding schemes for the OTN-BR and a promising research direction.

APPENDIX A
PROOF OF PROPOSITION 1

At the destination $d \in \mathcal{D}$, based on the received signals $\boldsymbol{Y}_{d,\mathcal{S}_d}$ and $\boldsymbol{Y}_{d,r}$, the MMSE estimation of the transmitted signal $X_s,\ s \in \mathcal{S}_d$ is given by:

$$\hat{x}_{s,d} = g_s\left(\boldsymbol{Y}_{d,\mathcal{S}_d}, \boldsymbol{Y}_{d,r}\right) = E\left[X_s | \boldsymbol{Y}_{d,\mathcal{S}_d}, \boldsymbol{Y}_{d,r}\right] = \sum_{I_{\mathcal{S}_d}} E\left[X_s | I_{\mathcal{S}_d}\right] P\left(I_{\mathcal{S}_d} | \boldsymbol{Y}_{d,\mathcal{S}_d}, \boldsymbol{Y}_{d,r}\right). \tag{19}$$

Since the sources are independent, we have $E\left[X_s | I_{\mathcal{S}_d}\right] = E\left[X_s | I_s\right]$ and from (19) we obtain

$$g_s\left(\boldsymbol{Y}_{d,\mathcal{S}_d}, \boldsymbol{Y}_{d,r}\right) = \sum_{I_{\mathcal{S}_d}} E\left[X_s | I_s\right] P\left(I_{\mathcal{S}_d} | \boldsymbol{Y}_{d,\mathcal{S}_d}, \boldsymbol{Y}_{d,r}\right). \tag{20}$$

Using Bayes' theorem, we have

$$P\left(I_{\mathcal{S}_d} | \boldsymbol{Y}_{d,\mathcal{S}_d}, \boldsymbol{Y}_{d,r}\right) = \frac{P\left(\boldsymbol{Y}_{d,\mathcal{S}_d}, \boldsymbol{Y}_{d,r} | I_{\mathcal{S}_d}\right) P(I_{\mathcal{S}_d})}{P\left(\boldsymbol{Y}_{d,\mathcal{S}_d}, \boldsymbol{Y}_{d,r}\right)}, \tag{21}$$

where

$$P\left(\boldsymbol{Y}_{d,\mathcal{S}_d}, \boldsymbol{Y}_{d,r} | I_{\mathcal{S}_d}\right) = P\left(\boldsymbol{Y}_{d,\mathcal{S}_d} | I_{\mathcal{S}_d}\right) P\left(\boldsymbol{Y}_{d,r} | I_{\mathcal{S}_d}\right). \tag{22}$$

Thus, using (21) and (22), equation (20) is rewritten as

$$g_s\left(\boldsymbol{Y}_{d,\mathcal{S}_d}, \boldsymbol{Y}_{d,r}\right) = \frac{\sum_{I_{\mathcal{S}_d}} E\left[X_s | I_s\right] P\left(\boldsymbol{Y}_{d,\mathcal{S}_d} | I_{\mathcal{S}_d}\right) P\left(\boldsymbol{Y}_{d,r} | I_{\mathcal{S}_d}\right) P(I_{\mathcal{S}_d})}{P\left(\boldsymbol{Y}_{d,\mathcal{S}_d}, \boldsymbol{Y}_{d,r}\right)}, \tag{23}$$

where

$$P\left(\boldsymbol{Y}_{d,r} | I_{\mathcal{S}_d}\right) = \sum_{I_r} P\left(\boldsymbol{Y}_{d,r} | I_r\right) P\left(I_r | I_{\mathcal{S}_d}\right). \tag{24}$$

Finally, using (23) and (24), we can obtain (2). Based on (22), the term $K = P\left(\boldsymbol{Y}_{d,\mathcal{S}_d}, \boldsymbol{Y}_{d,r}\right)$ is given by (3) as a factor normalizing the sum of probabilities to one.

APPENDIX B
PROOF OF PROPOSITION 3

Consider $\mathcal{D}_{\mathcal{F}} = \bigcup_{s\in\mathcal{F}} \mathcal{D}_s$, $\mathcal{S}_{\mathcal{A}} = \bigcup_{d\in\mathcal{A}} \mathcal{S}_d$ and $\boldsymbol{Y}_{\mathcal{A},\mathcal{F}} = \{\boldsymbol{Y}_{d,s} : d \in \mathcal{A},\ s \in \mathcal{F},\ (s,d) \in \mathcal{G}\}$, $\forall \mathcal{F} \subset S$ and $\forall \mathcal{A} \subset \mathcal{D}_{\mathcal{F}}$, where $\mathcal{G}$ is defined in (1). In view of the max-flow min-cut theorem [6] for the OTN-BR, an outer bound for the capacity region is the set of rate vectors $(R_{c,1}, R_{c,2}, \ldots R_{c,N})$ satisfying

$$\begin{aligned}\sum_{s\in\mathcal{F}} R_{c,s} \leq \min\{ & I\left(X_{\mathcal{F}}; \boldsymbol{Y}_{\mathcal{D}_{\mathcal{F}},\mathcal{F}}, \boldsymbol{Y}_{r,\mathcal{F}} | X_{\mathcal{F}^c}, X_r, Q\right), \\ & I\left(X_{\mathcal{F}}, X_r; \boldsymbol{Y}_{\mathcal{A},r}, \boldsymbol{Y}_{\mathcal{A},\mathcal{F}} | X_{\mathcal{F}^c}, Q\right) :\ \forall \mathcal{A} \subset \mathcal{D}_{\mathcal{F}},\ \mathcal{S}_{\mathcal{A}} \cap \mathcal{F} = \mathcal{F}\}\end{aligned} \tag{25}$$

over all distributions $P(Q)\left(\prod_{s=1}^{N} P(X_s|Q)\right) P\left(X_r|X_{\mathcal{S}},Q\right)$ with $|Q| \leq N+1$. Considering time-multiplexing in OTN-BR as described before, we have

$$\begin{aligned}\sum_{s\in\mathcal{F}} R_{c,s} \leq \max_{\substack{0\leq\lambda_{\acute{s}}\leq 1\\ \acute{s}\in\mathcal{S}}} \min\Bigg\{&\sum_{\acute{s}\in\mathcal{F}}\lambda_{\acute{s}} I\left(X_{\acute{s}};\boldsymbol{Y}_{\mathcal{D}_{\acute{s}},\{\acute{s}\}},\boldsymbol{Y}_{r,\acute{s}}|Q\right),\\ &\sum_{\acute{s}\in\mathcal{F}}\lambda_{\acute{s}} I\left(X_{\acute{s}};\boldsymbol{Y}_{\mathcal{A},\{\acute{s}\}}|Q\right)+\left(1-\sum_{\acute{s}\in\mathcal{S}}\lambda_{\acute{s}}\right) I\left(X_r;\boldsymbol{Y}_{\mathcal{A},\{r\}}|Q\right):\ \forall\mathcal{A}\subset\mathcal{D}_{\mathcal{F}},\ \mathcal{S}_{\mathcal{A}}\cap\mathcal{F}=\mathcal{F}\Bigg\}.\end{aligned} \tag{26}$$

For Gaussian channels, the mutual information terms in (26) are maximized when the distributions of $X_k,\ k\in\{\mathcal{S}\cup\{r\}\}$ are Gaussian. Noting that in the considered settings we have $\max_{P(X_k)} I\left(X_k;\boldsymbol{Y}_{\mathcal{B},\{k\}}\right)=\frac{1}{2}\log_2\left(1+\sum_{\substack{j\in\mathcal{B},\\(k,j)\in\mathcal{G}}}\frac{P_k}{\sigma_{k,j}^2}\right)$, where $\mathcal{B}\subset\{\mathcal{D}\cup\{r\}\}$ and $k\in\{\mathcal{S}\cup\{r\}\}$ [6], the proof of Proposition 3 is complete.

REFERENCES

[1] G. Kramer, M. Gastpar, and P. Gupta, "Cooperative strategies and capacity theorems for relay networks," *IEEE Trans. Inform. Theory*, vol. 51, no. 9, pp. 3037–3063, Sep. 2005.

[2] Y. Liang, "Multiuser communications with relaying and user cooperation," Ph.D. dissertation, Dep. Elec. Comp. Eng., Univ. Illinois at Urbana-Champaign, Urbana, IL, USA, 2005.

[3] A. Tajer and A. Nosratinia, "A broadcasting relay for orthogonal multiuser channels," in *IEEE GLOBECOM*, San Francisco, CA, Nov. 2006, pp. 1–5.

[4] R. Krishna, Z. Xiong, and S. Lambotharan, "A cooperative MMSE relay strategy for wireless sensor networks," *IEEE Signal Process. Lett.*, vol. 15, pp. 549–552, Jul. 2008.

[5] O. Sahin and E. Erkip, "Achievable rates for the Gaussian interference relay channel," in *IEEE GLOBECOM*, Washington D.C., USA, Nov. 2007, pp. 1627–1631.

[6] T. M. Cover and J. A. Thomas, *Elements of Information Theory*. New York: Wiley, 1991.

[7] E. Tuncel, "Slepian-wolf coding over broadcast channels," *IEEE Trans. Inform. Theory*, vol. 52, no. 4, pp. 1469–1482, Apr. 2006.

[8] Q. Li, S. H. Ting, and C. K. Ho, "Nonlinear network code for high throughput broadcasting with retransmissions," in *IEEE Int. Symp. Inform. Theory*, Seoul, Korea, Jun. 2009, pp. 2853–2857.

[9] J. Karlsson and M. Skoglund, "Joint source-channel mappings for the relay channel," in *IEEE Int. Conf. Acoust., Speech and Signal Process.*, Las Vegas, Nevada, USA, Apr. 2008, pp. 2953–2956.

[10] K. S. Gomadam and S. A. Jafar, "Optimal relay functionality for SNR maximization in memoryless relay networks," *IEEE J. Sel. Areas Commun.*, vol. 25, no. 2, pp. 390–401, Feb. 2007.

[11] I. Abou-Faycal and M. Medard, "Optimal uncoded regeneration for binary antipodal signaling," in *IEEE Int. Conf. Commun.*, Paris, France, Jun. 2004, pp. 742–746.

[12] T. Cui, T. Ho, and J. Kliewer, "Memoryless relay strategies for two-way relay channels," *IEEE Trans. Commun.*, vol. 57, no. 10, pp. 3132–3143, Oct. 2009.

[13] IEEE 802.15.4 Standard Part 15.4: Wireless Medium Access Control (MAC) and Physical Layer (PHY) Specifications for Low-Rate Wireless Personal Area Networks (LR-WPANs), 2003.

[14] IEEE 802.15.1 Standard Part 15.1: Wireless Medium Access Control (MAC) and Physical Layer (PHY) Specifications for Wireless Personal Area Networks (WPANs), 2002.

[15] R. Ahlswede, N. Cai, S.-Y. R. Li, and R. W. Yeung, "Network information flow," *IEEE Trans. Inform. Theory*, vol. 46, no. 4, pp. 1204–1216, Jul. 2000.

[16] S.-Y. R. Li, R. W. Yeung, and N. Cai, "Linear network coding," *IEEE Trans. Inform. Theory*, vol. 49, no. 2, pp. 371–381, Feb. 2003.

[17] M. Effros, M. Medard, S. R. T. Ho, D. Karger, and R. Koetter, "Linear network codes: a unified framework for source, channel and network coding," in *DIMACS Workshop Network Inform. Theory*, Piscataway, NJ, Mar. 2003.

[18] A. Ramamoorthy, K. Jain, P. A. Chou, and M. Effros, "Separating distributed source coding from network coding," *IEEE Trans. Inform. Theory*, vol. 52, no. 6, pp. 2785–2795, Jun. 2006.

[19] N. Cai and R. W. Yeung, "Network coding and error correction," in *IEEE Inform. Theory Workshop*, Bangalore, India, Oct. 2002, pp. 119–122.

[20] R. Koetter and F. R. Kschischang, "Coding for errors and erasures in random network coding," *IEEE Trans. Inform. Theory*, vol. 54, no. 8, pp. 3579–3591, Aug. 2008.

[21] H. Bahramgiri and F. Lahouti, "Block network error control codes and syndrome-based maximum likelihood decoding," in *IEEE Int. Symp. Inform. Theory*, Toronto, ON, Canada, Jul. 2008, pp. 807 – 811.

[22] C. Hausl and P. Dupraz, "Joint network-channel coding for the multiple-access relay channel," in *IEEE Commun. Society Conf. on Sensor, Mesh and Ad Hoc Commun. and Networks*, Reston, VA, USA, Sep. 2006, pp. 817 – 822.

[23] R. K. S. Yang, "Network coding over a noisy relay: A belief propagation approach," in *IEEE Int. Symp. Inform. Theory*, Nice, France, Jun. 2007, pp. 801 – 804.

[24] L. Xiao, T. E. Fuja, J. Kliewer, and D. J. Costello, Jr., "Nested codes with multiple interpretations," in *40th Annual Conference on Information Sciences and Systems*, Princeton, NJ, Mar. 2006, pp. 851 – 856.

[25] J. Kliewer, T. Dikaliotis, and T. Ho, "On the performance of joint and separate channel and network coding in wireless fading networks," in *IEEE Inform. Theory Workshop on Information Theory for Wireless Networks*, Solstrand, Jul. 2007, pp. 1–5.

[26] A. Host-Madsen and J. Zhang, "Capacity bounds and power allocation for the wireless relay channel," *IEEE Trans. Inform. Theory*, vol. 51, no. 6, pp. 2020–2040, Jun. 2005.

[27] F. Lahouti and A. K. Khandani, "Efficient source decoding over memoryless noisy channels using higher order markov models," *IEEE Trans. Inform. Theory*, vol. 50, no. 9, pp. 2103–2118, Sep. 2004.

[28] N. Farvardin, "A study of vector quantization for noisy channels," *IEEE Trans. Inform. Theory*, vol. 36, no. 4, pp. 799–809, Jul. 1990.

[29] A. A. E. Gamal, L. A. Hamachandra, I. Shperling, and V. Wei, "Using simulated annealing to design good codes," *IEEE Trans. Inform. Theory*, vol. 33, no. 1, pp. 116–123, Jan. 1987.

[30] S. Heinen and P. Vary, "Source-optimized channel coding for digital transmission channels," *IEEE Trans. Commun.*, vol. 53, no. 4, pp. 592–600, Apr. 2005.

[31] E. Agrell, A. Vardy, and K. Zeger, "A table of upper bounds for binary codes," *IEEE Trans. Inform. Theory*, vol. 47, no. 7, pp. 3004–3006, Nov. 2001.

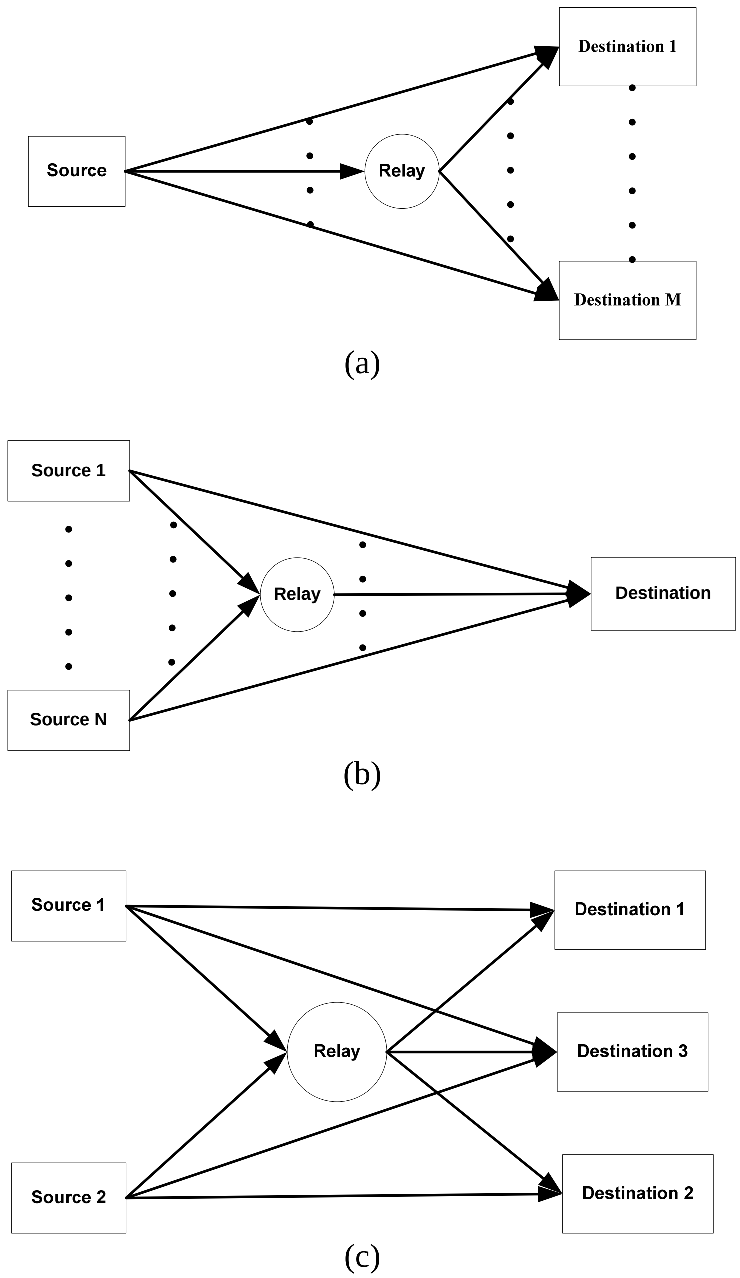

Fig. 1. (a) BRC (b) MARC and (c) TN-BR-(2,3).

6	6	6	6	4	4	4	4
6	6	6	6	4	4	4	4
5	6	6	3	0	4	4	7
5	5	3	3	0	0	7	7
5	5	3	3	0	0	7	7
5	5	2	2	1	1	7	7
5	2	2	2	1	1	1	7
2	2	2	2	1	1	1	1

(a)

6	6	6	6	4	4	4	4
6	6	6	6	4	4	4	4
5	5	3	3	0	0	7	7
5	5	3	3	0	0	7	7
5	5	3	3	0	0	7	7
5	5	3	3	0	0	7	7
2	2	2	2	1	1	1	1
2	2	2	2	1	1	1	1

(b)

Fig. 2. Nonlinear network codes for an OTN-BR with $N = 2$ and $SNR_{sr} = 10\text{dB}$, (a) using DNNC-C4 and (b) structured network coding.

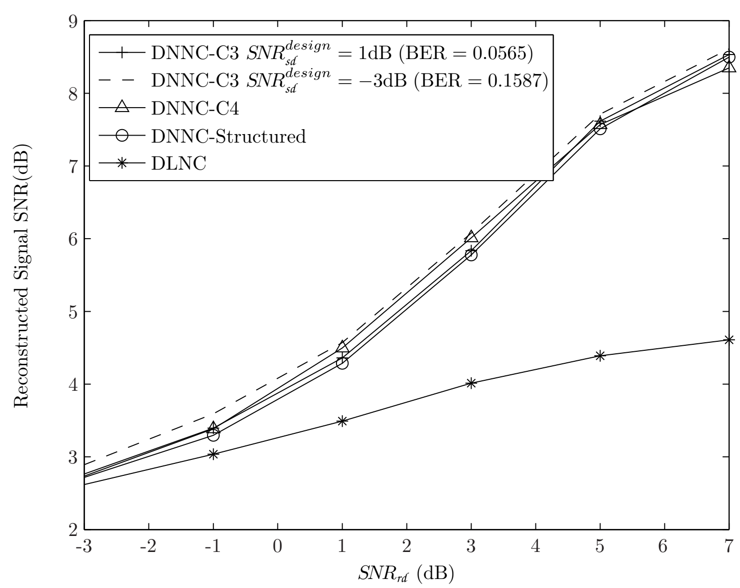

Fig. 3. Performance of the proposed DNNC and DLNC for an OMC-BR with two sources, $R_r = R = 3$, $SNR_{sr} = 10\text{dB}$ and $SNR_{sd} = -3\text{dB}$.

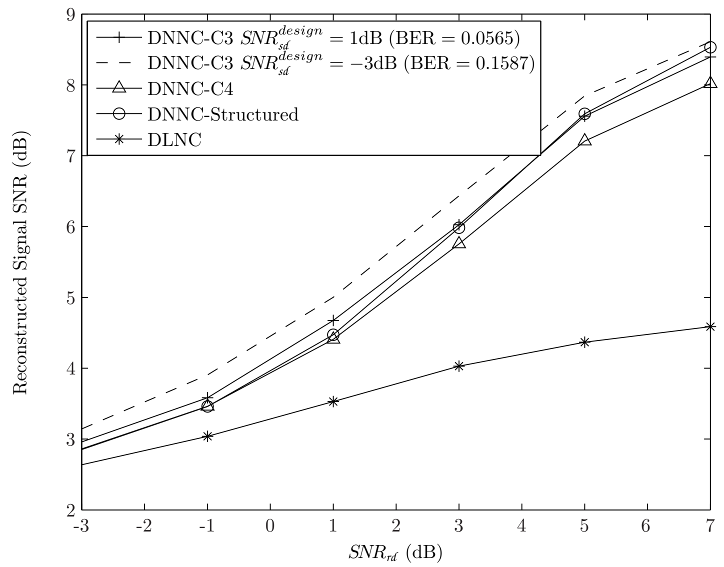

Fig. 4. Performance of the proposed DNNC and DLNC for an OMARC with two sources, $R_r = R = 3$, $SNR_{sr} = 10$dB and $SNR_{sd} = -3$dB.

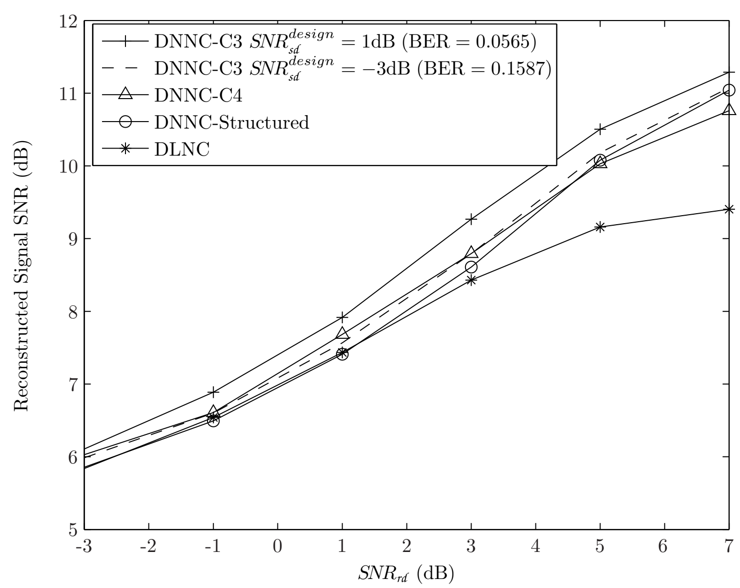

Fig. 5. Performance of the proposed DNNC and DLNC for an OMARC with two sources, $R_r = R = 3$, $SNR_{sr} = 10$dB and $SNR_{sd} = 1$dB.

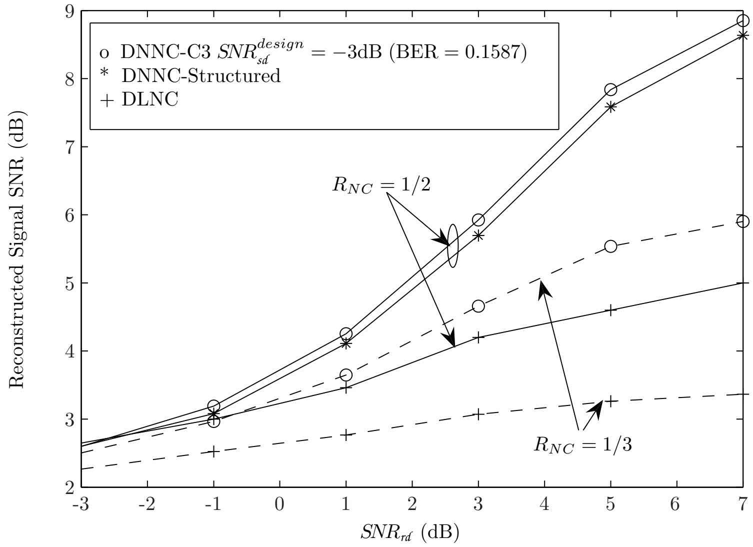

Fig. 6. Performance of the proposed DNNC and DLNC for an OMC-BR with three sources, $SNR_{sr} = 10$dB and $SNR_{sd} = -3$dB.

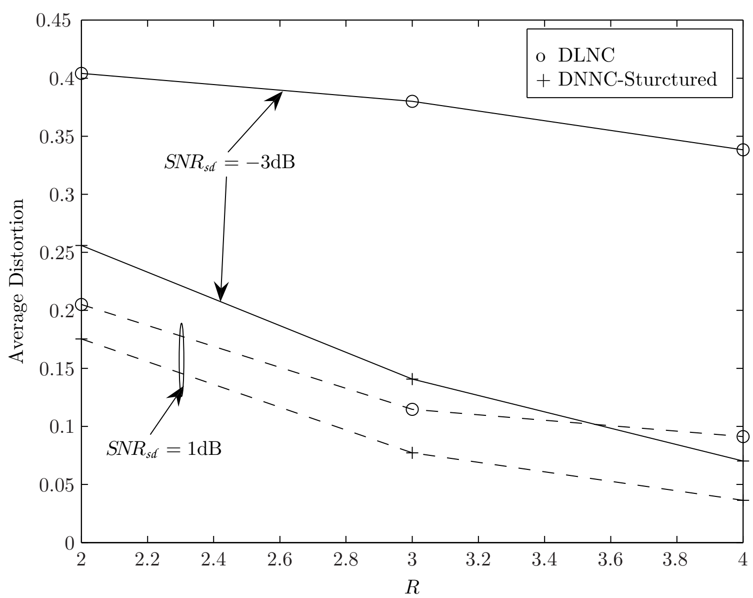

Fig. 7. Average distortion vs. rate for an OMARC with two sources, $R_r = R$, $SNR_{sr} = 10$dB and $SNR_{rd} = 7$dB.

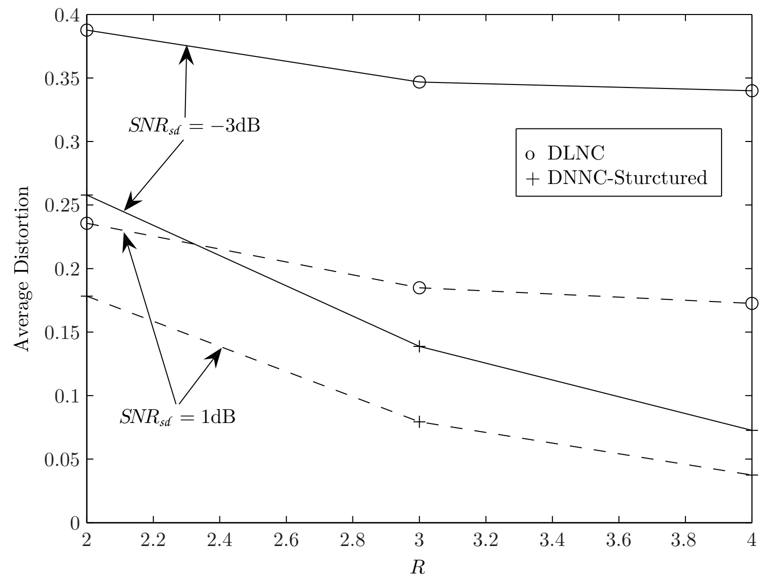

Fig. 8. Average distortion vs. rate for an OTN-BR-(2,3) with $R_r = R$, $SNR_{sr} = 10$dB and $SNR_{rd} = 7$dB.

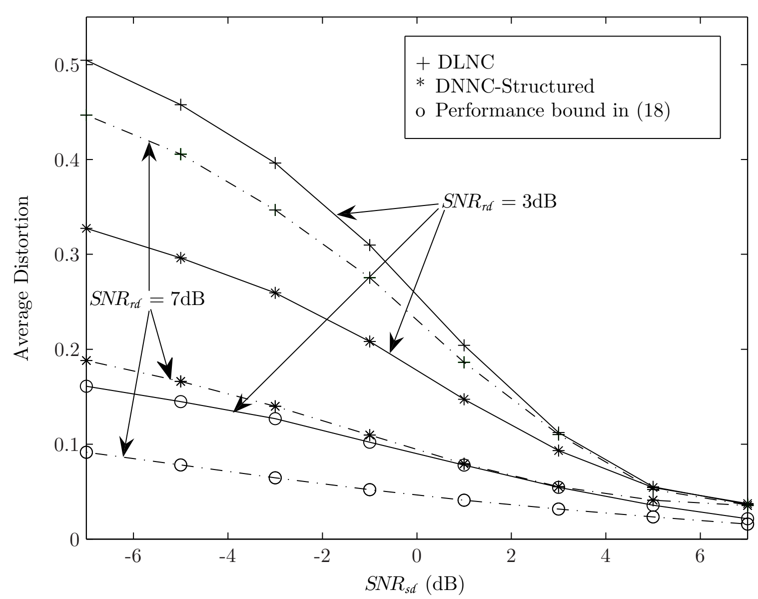

Fig. 9. Average distortion vs. source-destination channel SNR for an OTN-BR-(2,3) with two sources, $R_r = R = 3$ and $SNR_{sr} = 10$dB. Performance of linear and proposed structured nonlinear network coding at the relay in comparison with the performance bound in (18).